The Effect of Spinning Speed and Drawing Temperature on Structure and Properties of Poly(ethylene Terephthalate) Yarns

R. HUISMAN and H. M. HEUVEL, *Enka bv Research Institute, Arnhem, The Netherlands*

Synopsis

From an industrial point of view, it is effective to have a relation between process conditions and resulting product properties. In practice there are many possible process conditions, whereas properties are generally interrelated in a complex way. Thus, there is a strong need for a physical understanding of the product properties in terms of process settings. This comprehension should also allow one to predict possible consequences for the properties when new process conditions become available. To obtain that physical understanding for the development of production processes of PET yarns, use has been made of a simple two-phase model of crystalline and amorphous regions. As process parameters the spinning speed and the drawing temperature were chosen. As the drawing temperatures are only known as machine-setting values, they are simply referred to as "low" and "high." As mechanical properties the shrinkage, modulus, tenacity, and dynamic mechanical behavior are discussed.

INTRODUCTION

A synthetic yarn process essentially is a succession of polymer and yarn treatments using combinations of temperature, tension, and residence time. Almost all process conditions can be translated into these three variables. For a given polymer the combination of process conditions completely determines the thermal and mechanical properties of the yarns produced. The way in which process conditions influence the yarn properties, and hence the relation between the two, is highly relevant with respect to process control or process development.

If, for a given end use, a yarn with a particular combination of properties is required, knowledge of the relations just mentioned permits the translation of these product requirements into a set of appropriate process conditions. In this way this knowledge can guide the process development effectively. Moreover, for subsequent process control it will prove to be of high practical importance.

The relation just mentioned, however, generally is not a simple one. All separate steps have their own (mostly interdependent) conditions. Relating the yarn properties to this set of process conditions makes relationships of this kind often obscure and very complicated. In this situation a good insight into the physical yarn structure is helpful. The physical structure can be regarded as an intermediate between yarn process and yarn properties. This is schematically illustrated in Figure 1. A set of process conditions results in a physical yarn structure that is responsible for the intrinsic yarn properties. With

Journal of Applied Polymer Science, Vol. 37, 595–616 (1989)
 CCC 0021-8995/89/030595-22$04.00

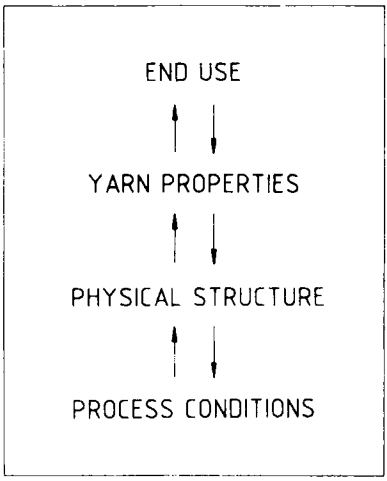

Fig. 1. Intermediate position of the physical yarn structure.

respect to the physical structure, two types of relation can therefore be distinguished, viz.:

(a) relations between process conditions and physical yarn structure;
(b) relations between structure and yarn properties.

In this way the relations observed can be interpreted in physical terms. This improves not only their own reliability, but also the reliability of process extrapolations. Another advantage is that via the physical structure the interrelation between the yarn properties is more easily recognized and better understood.

In recent years there has been a growing interest in the study of physical fiber structure. This may be ascribed to an increased need for high-quality fibers and the aim to produce these fibers with high economic efficiency. One of the ways to meet the efficiency requirement is to apply drastically increased process speeds. To study the influence of this parameter, the choice fell on a set of yarns wound at a variety of speeds and drawn at two different temperature levels. Especially the yarns wound at increased speeds can be regarded as representative of a new generation of industrial yarns. A characteristic of these yarns is a favorable combination of mechanical properties with respect to several end uses, viz., lower shrinkage, higher modulus, and an improved fatigue resistance at the expense of a somewhat reduced tenacity.

In this paper this new combination of properties is discussed in terms of the specific physical structure of these high speed spun samples. As only the drawn yarns are of commercial interest, we have confined our description to these samples. Characteristics of the undrawn yarns have been published earlier by several authors.

Finally, the results to be presented should not be considered as general relations as they also depend on processing details which, we think, are not relevant within the scope of this paper. Our ultimate goal is to illustrate how structure work can be applied for effective process development.

GENERAL PHYSICAL YARN MODEL AND BRIEF DISCUSSION OF CHARACTERIZATION

A general structural model of an oriented PET fiber is given in Figure 2. It can be seen that ordered (crystalline) regions alternate with less ordered (amorphous) domains. The picture also shows that a single molecule may run through several crystalline and amorphous regions. Besides, there is the possibility that a molecule folds back on the surface of a crystal to reenter it. Depending upon the process conditions, the polymer molecules are more or less oriented along the fiber axis. In this way, so-called fibrils are formed, i.e., structural units in which the coherence of amorphous and crystalline domains is found, predominantly in the longitudinal direction. However, these fibrils also have a lateral extension, as indicated in Figure 2.

The most important characteristics of the physical structure are the crystallinity, size, and orientation of the crystals, and for the amorphous regions their size as well as the orientation of the molecules in these regions. Wide angle x-ray diffraction is used to obtain information about the crystalline morphology (crystal sizes and packing of the molecules in the crystals). The combination of x-ray diffraction and overall density measurement yields the crystallinity. Combined results of pulse propagation, crystallinity, and crystalline orientation, finally, yield an estimate of the amorphous orientation. A schematic survey of the procedure outlined above is given in Figure 3, more detailed information being given in the literature.[1,2]

In the preceding section it was mentioned that this kind of analysis has to be applied for process development. Therefore, at least two requirements can

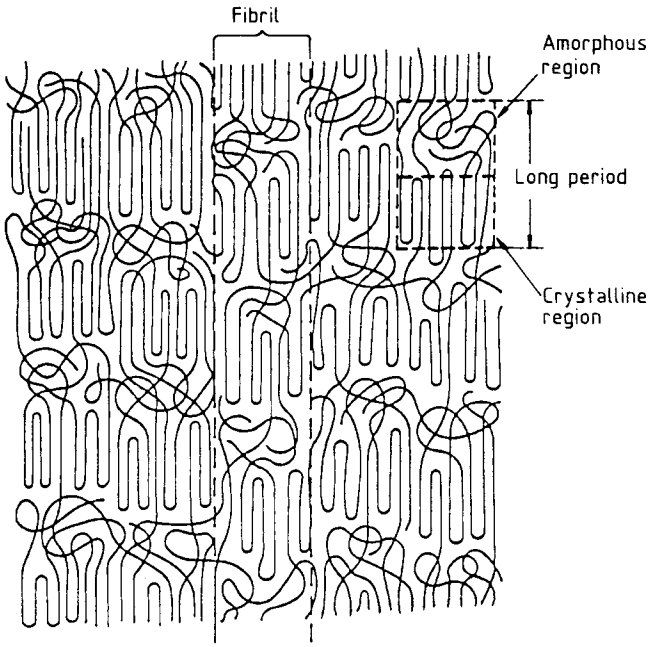

Fig. 2. Structural model of drawn PET yarn.

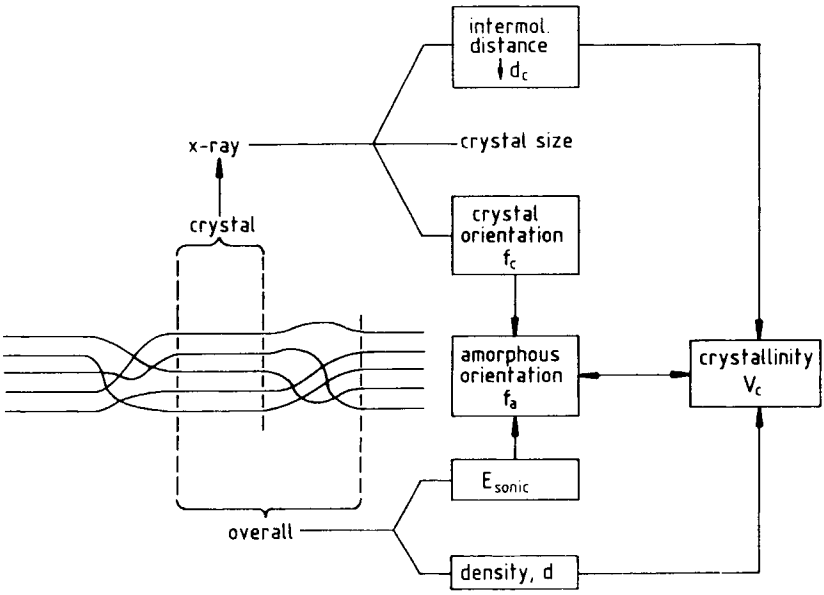

Fig. 3. Schematic representation of a combination of structural characterization techniques.

be formulated:

1. The information must be accurate and quantitative in order to permit a comparison between data of yarns that do not differ too much.
2. The methods must be quick in order to establish in that process development a rapid feedback from yarn structure to process conditions.

With respect to x-ray diffraction, these requirements can be met by means of a highly automated procedure in which curve resolution is applied to experimental diffractometer scans. An example of such a scan is given in Figure 4, showing an equatorial x-ray trace of a polyester yarn. As can be seen, this scan is composed of three rather sharp crystalline reflections and one broad line, brought about by the scattering of the amorphous regions. The experimental profile is fitted to the sum of four symmetrical bell-shaped lines. The fitting yields parameters such as peak position and half-widths that can be translated into morphological parameters such as molecular distances and crystal sizes.

The bell-shaped function used in the fitting procedure is a so-called Pearson VII function, which is applied by us for several purposes. It is governed by the combination of four parameters, i.e., peak height, peak position and two parameters describing the half-width and the shape of the curve at the tail. This latter effect is shown in Figure 5, where plots of the function are given for different values of the shape parameter, at the same half-width. In this way the most important advantage of the Pearson VII function is shown: The half-width and the tail of the distribution can be varied independently, a property not possessed by more conventional functions, often applied in this field, such as Gauss and Lorentz functions. As a matter of fact, the latter two curves are special cases of the Pearson VII curve with m values being infinite or 1, respectively.

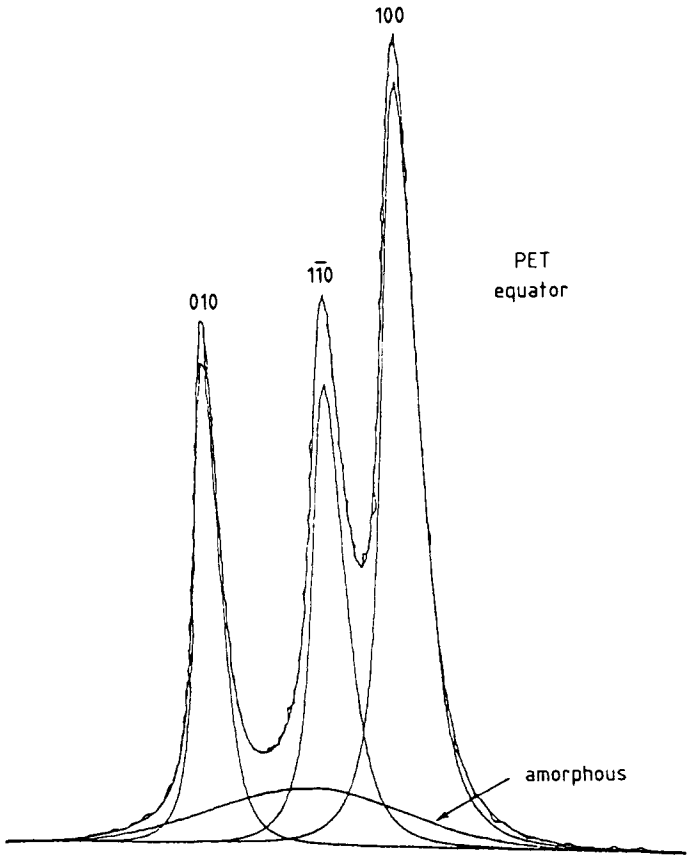

Fig. 4. Profile and deconvolution of an equatorial x-ray scan of PET.

RELATION BETWEEN PHYSICAL STRUCTURE AND MECHANICAL PROPERTIES

Yarn Samples

Having established the structural characteristics, a trial can be made to describe the mechanical yarn properties in terms of these parameters. By way of illustration, use is made of a series of yarns spun at speeds ranging from 1000 to 5000 m/min (spinning temperature 300°C, orifice diameter 500 μm), and drawn at two different temperatures, one at a moderate level, the other rather close to the melting point, to a residual elongation at break of about 10%. The yield is adjusted in such a way that the drawn yarns have a constant diameter (1100 dtex, 210 filaments). The molecular weight of the yarns, M_n, was about 30,000.

Shrinkage

As dimensional stability is a highly relevant characteristic of industrial yarns, it seems appropriate first to show how shrinkage can be described in terms of structural parameters.

In Figure 6 the hot air shrinkage at 160°C (HAS 160) of the drawn yarns, measured at a load of 0.5 cN/tex, is plotted vs. the spinning speed. A

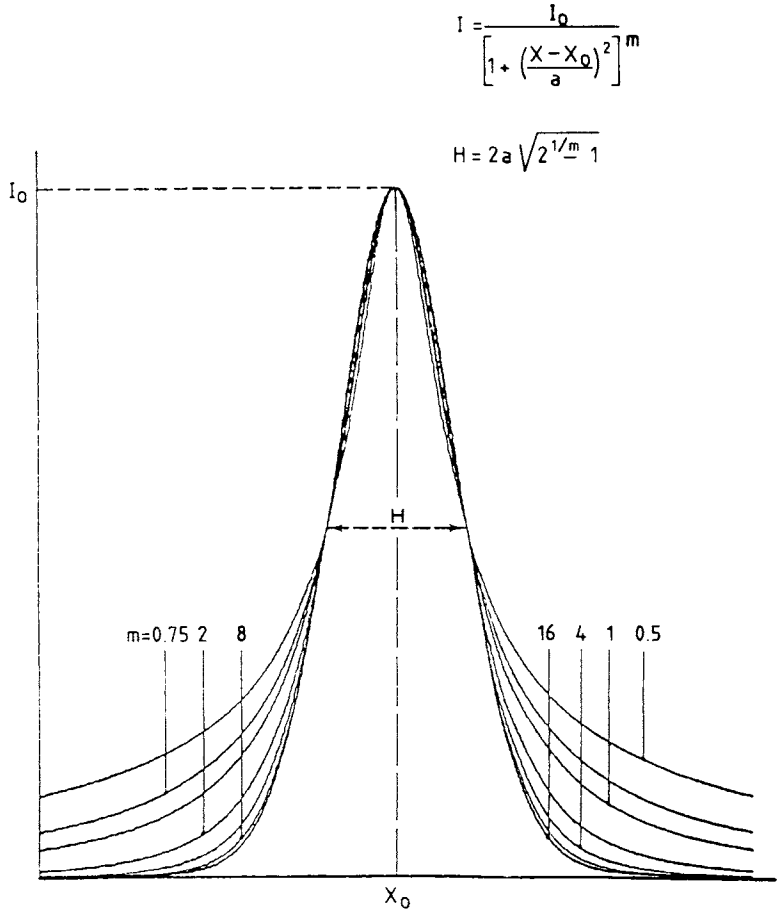

Fig. 5. Properties of the Pearson VII function.

decreasing shrinkage is observed at increasing spinning speed, while in addition a significantly lower shrinkage is found for the yarns drawn at the higher temperature. This behavior is discussed in terms of structural parameters of the two-phase model as presented in Figure 2. The driving force behind yarn shrinkage is of entropic nature. Above the glass-transition temperature, the polymer molecules in the amorphous domains have sufficient mobility to obtain their most probable configuration, which means that they will tend to coil up. The higher the temperature, the more pronounced this process will be. Contrary to this behavior is that of the crystals. In most cases, the crystals may be regarded to behave as rigid blocks during the thermal shrinkage. Based on these arguments, the yarn shrinkage can be expected to be proportional to the amount of amorphous material, to be described by the factor $(1 - V_c)$. The second factor governing the yarn shrinkage is the orientation of the molecular segments in the amorphous domains. In the unstrained condition a well-oriented segment is a configuration of low statistical probability. Therefore, it will have a pronounced tendency to coil up, which means that a high amorphous orientation will give rise to a large disorientation, resulting in

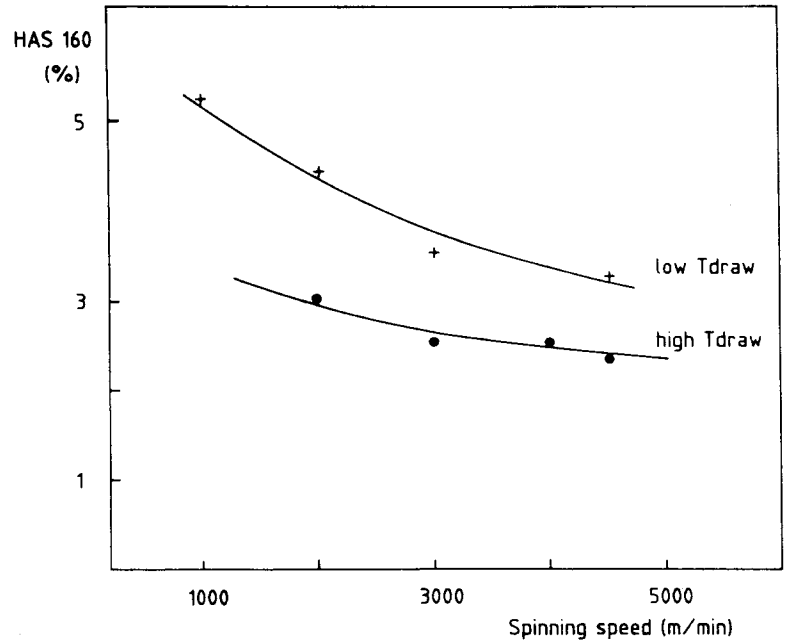

Fig. 6. Hot air shrinkage of drawn yarns spun at various speeds and drawn at two different temperatures.

a high shrinkage. A combination of both arguments provides the quantity $(1 - V_c)f_a$, which can be tried for describing the shrinkage behavior of a yarn.

Now, these considerations will be applied to the present series of yarns. Figure 7 shows the plot of the shrinkage of the drawn yarns vs. the value of $(1 - V_c)f_a$. From this plot it is clear that the shrinkage is a unique function of

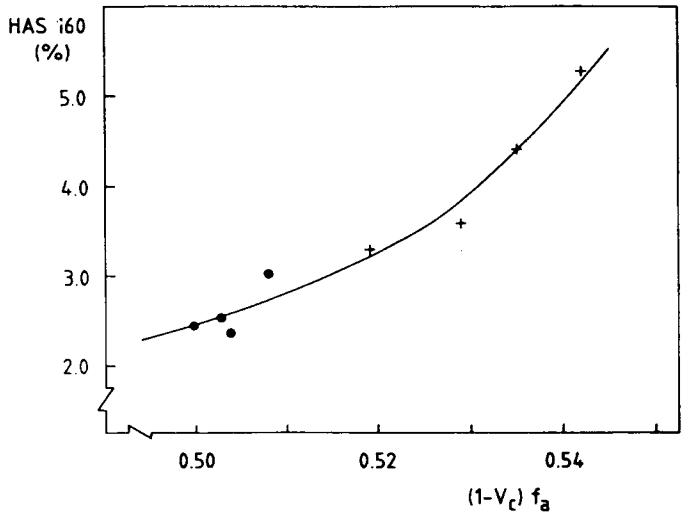

Fig. 7. Relation between hot air shrinkage and structural parameters: (●) high T_{draw}; (+) low T_{draw}.

the amount of amorphous material and its orientation factor. So it can be concluded that the shrinkage can be decreased either by increasing the crystallinity or decreasing the amorphous orientation. The application of high spinning speeds causes an appreciable increase in crystallinity of the undrawn yarns.[3] As this difference in crystallinity does not vanish completely during drawing, higher crystallinities are typical of high-speed spun yarns.[4] So, the low shrinkage values can mainly be ascribed to a relatively low amount of amorphous material.

Modulus

The second mechanical yarn characteristic which can be described in terms of the physical structure is the modulus. When a yarn is loaded in a stress–strain experiment, the load is exerted both on the crystals and on the molecules in the amorphous domains. As a first approximation, it is assumed that a high orientation results in a high modulus. This means that in the case of high orientation a deformation to a certain elongation will require a relatively high stress. Bearing in mind that both crystalline and amorphous regions are involved, a useful parameter could be the overall orientation factor, i.e., the crystalline and amorphous orientation factor weighed by the crystallinity:

$$f_o = V_c f_c + (1 - V_c) f_a$$

A useful way to describe the tensile behavior of a yarn is by plotting the modulus–strain curve, i.e., the first derivative of the stress–strain curve.[5] An example of a stress–strain curve and its corresponding modulus–strain analogue are given in Figure 8. Two peaks can be distinguished in the modulus–strain curve, the position and peak height of which change with the process conditions. The first peak occurs at very low elongations. In Figure 9 the height of this first peak is plotted vs. the overall orientation factor just mentioned. Examining the overall orientation factor proposed, an increasing crystallinity at constant amorphous and crystalline orientation results in an increase in overall orientation and, consequently, an increase in modulus. This is, in fact, the main reason for the increase in modulus with spinning speed, since high speed spun yarns exhibit higher crystallinities.

Details of the Amorphous Regions and Possible Consequences for Tenacity

For the description of shrinkage and modulus use has been made of information obtained in an indirect way about the amorphous regions. By means of combined knowledge of overall and crystalline orientation, conclusions about the amorphous orientation are drawn. As the structure in the amorphous domains is supposed to be highly significant to the mechanical behavior of a yarn, an attempt was made to gain a more detailed insight into that structure. Two features are supposed to be of major importance. The first is the folding of the molecules at the boundaries of the crystals. As folded chains cannot contribute to modulus or tenacity, they should be avoided as much as possible.

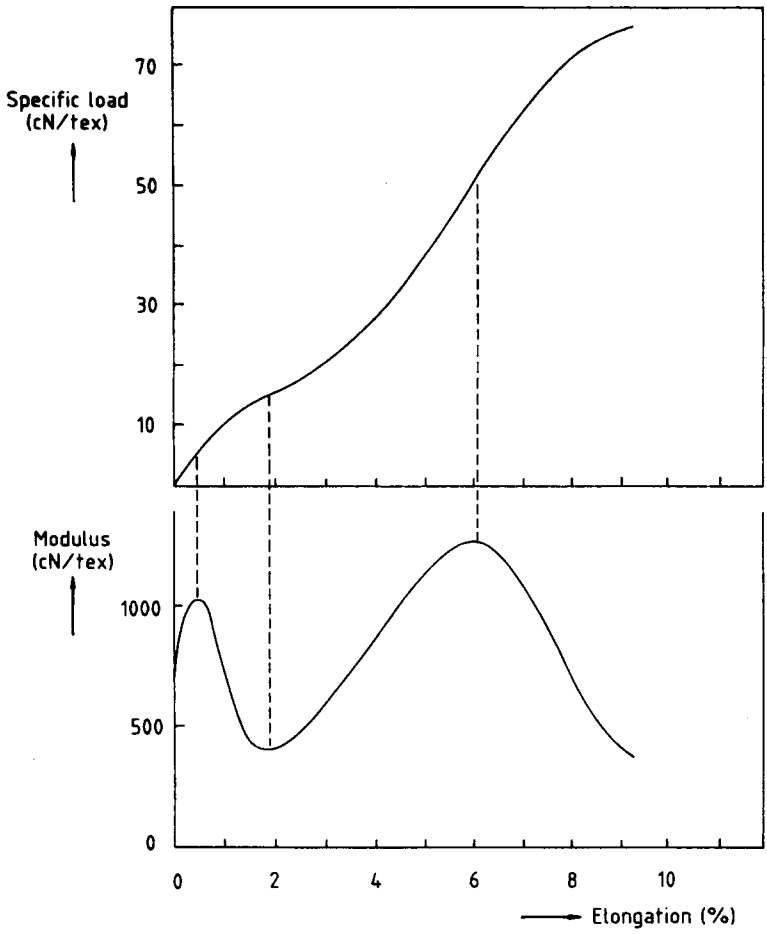

Fig. 8. Stress–strain and corresponding modulus–strain curve.

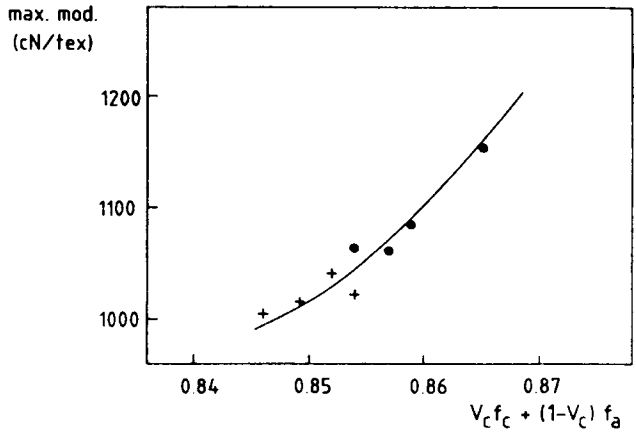

Fig. 9. Relation between initial modulus (first maximum in modulus-strain curve) and structural parameters: (●) high T_{draw}; (+) low T_{draw}.

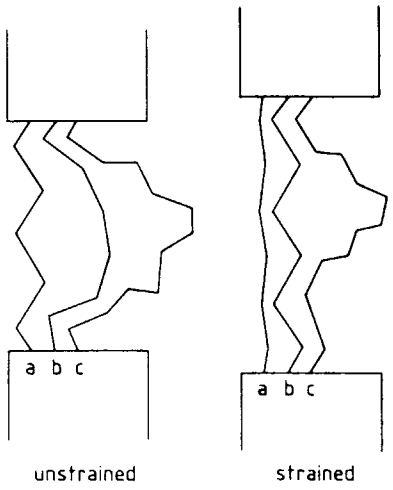

Fig. 10. Response of different tie molecules to straining.

The second is the tie-chain length distribution. Tie molecules are running from one crystal to the other. They may consist of many or of only a few monomer units. If the length distribution is broad, the molecules will not cooperate in bearing a load exerted on the yarn. This is schematically illustrated in Figure 10. Successive breakage or slippage of one molecule after the other will take place, resulting in lower strength and modulus. From the literature, evidence has emerged that infrared spectroscopy is able to provide information on these two structural features.[4,6,7] A spectrum of a PET yarn in the region 1100–700 cm^{-1} is shown in Figure 11. The shoulder at 989 cm^{-1} is ascribed by Statton et al. to the reentry of PET molecules in the crystal, the so-called fold band.[6]

The study of the tie-chain length distribution is much more complicated. Helpful in this respect is the fact that the glycol part of the PET molecule may occur in two different conformational states, i.e., trans and gauche (or cis), which can be distinguished by infrared analysis, as shown by Ward et al.[8–10] The bands involved are indicated in Figure 11.

In Figure 12 an illustration of the two conformers is given. As shown in this figure, the trans conformer is related to the straight parts of the molecule and both gauche conformers to the bended parts. Therefore, the reaction of the gauche content on elongation provides information on the uncoiling of the molecules in the amorphous regions. If uncoiling hardly takes place during elongation, long loose loops must be present, and the tie-chain length distribution is broad.

Finally, elongation cannot only cause uncoiling, indicated by gauche–trans transitions, but also tension on the taut tie molecule. According to several authors,[4,7,11] the increase in tension on these molecules is reflected in a shift of the 972 cm^{-1} band. This is also indicated in Figure 11. To obtain accurate and quantitative information from the IR spectrum, use was made of curve resolution. Spectra made with polarized infrared radiation parallel and perpendicular to the fiber axis are fitted simultaneously to a computer model describing the absorbance as the sum of a number of Pearson VII lines.

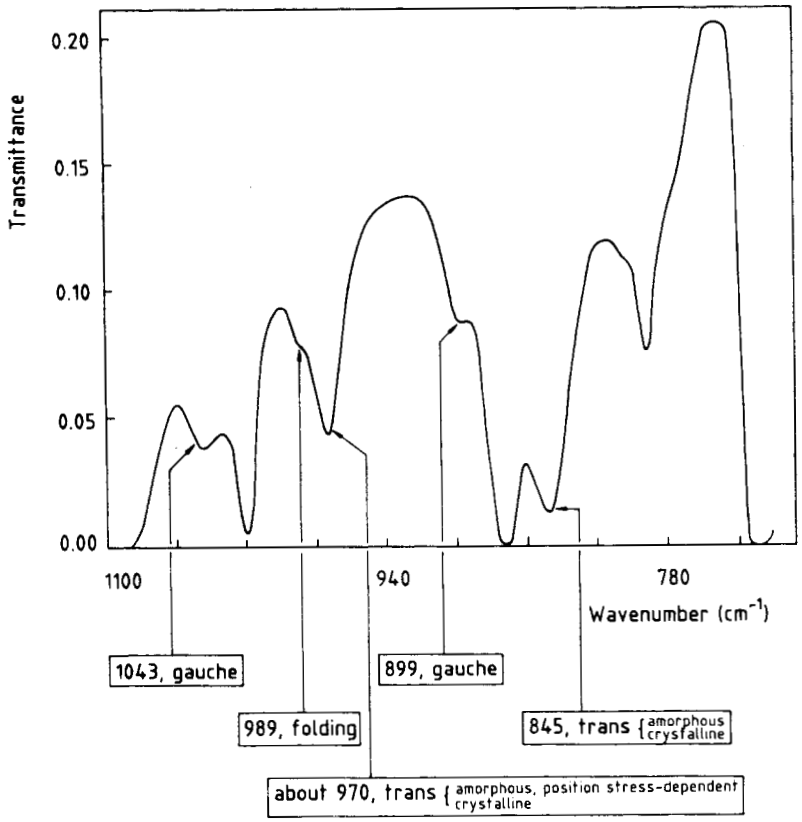

Fig. 11. IR spectrum of PET with some band assignments.

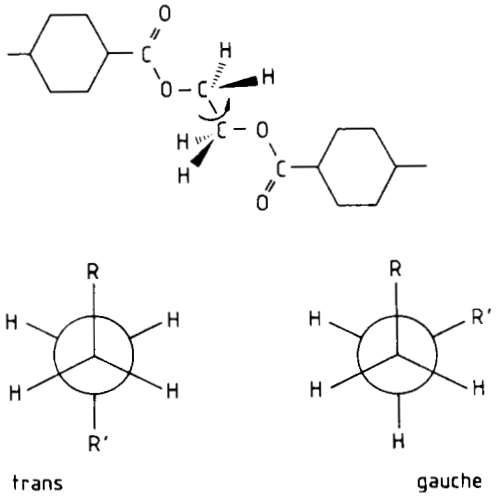

Fig. 12. Trans and gauche conformers of PET.

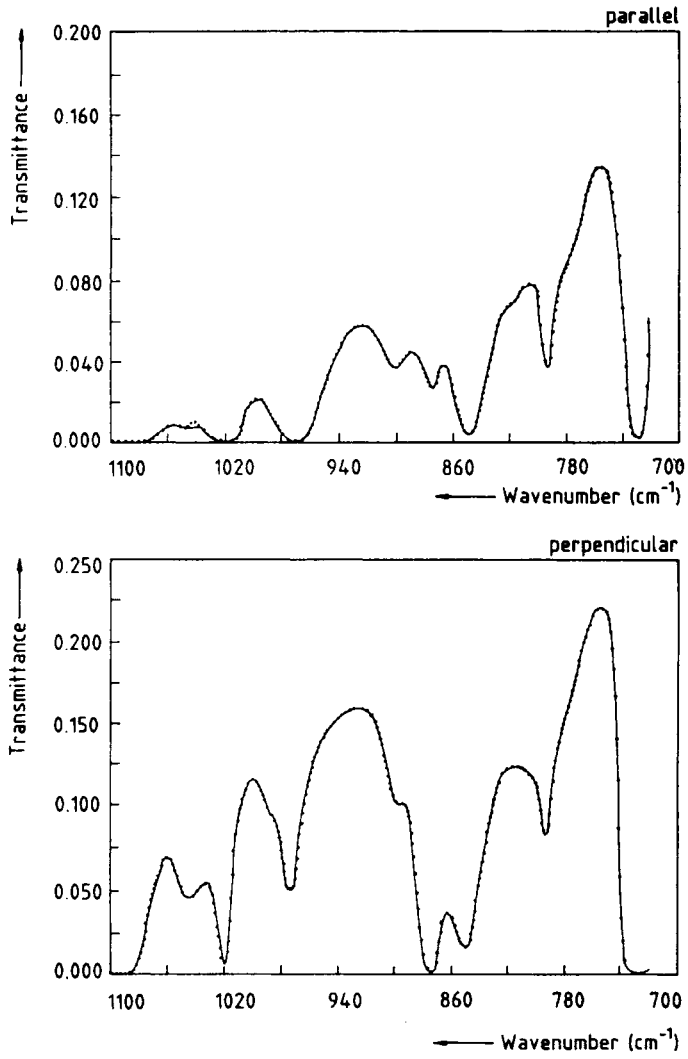

Fig. 13. Fitting results of parallel and perpendicular spectrum of a PET tyre yarn: (· · ·) experimental values; (—) fitted model.

Details of this procedure are given elsewhere.[4] An example of the fitting is presented in Figure 13.

Some results of the infrared analysis on the yarn series investigated are presented in the following figures: Figure 14 shows the fold content of yarns spun at various speeds and drawn at two temperatures. A definite increase in chain folding is observed at increased spinning speed and increased drawing temperature. In Figure 15 the concentration of gauche conformers in the amorphous domains is plotted for the drawn yarns vs. the spinning speed. From the figure it is clear that an increase in spinning speed results in a yarn with more *gauche* conformers in the amorphous regions. Figure 16 shows the course of the gauche content with elongation for two yarns spun at quite different speeds. To that end, IR samples have been wound at various elongations. The decrease of the gauche content for the yarn spun at 1000

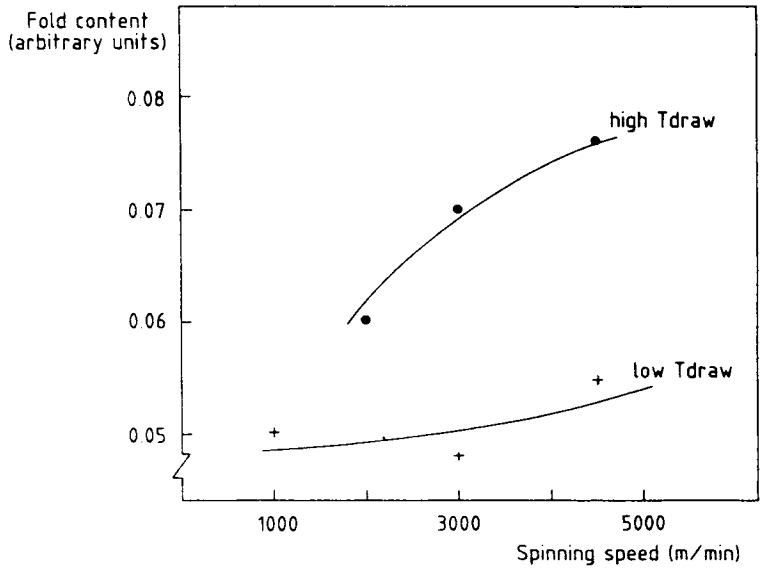

Fig. 14. Amount of chain folds for yarns spun at various speeds and drawn at two different temperatures.

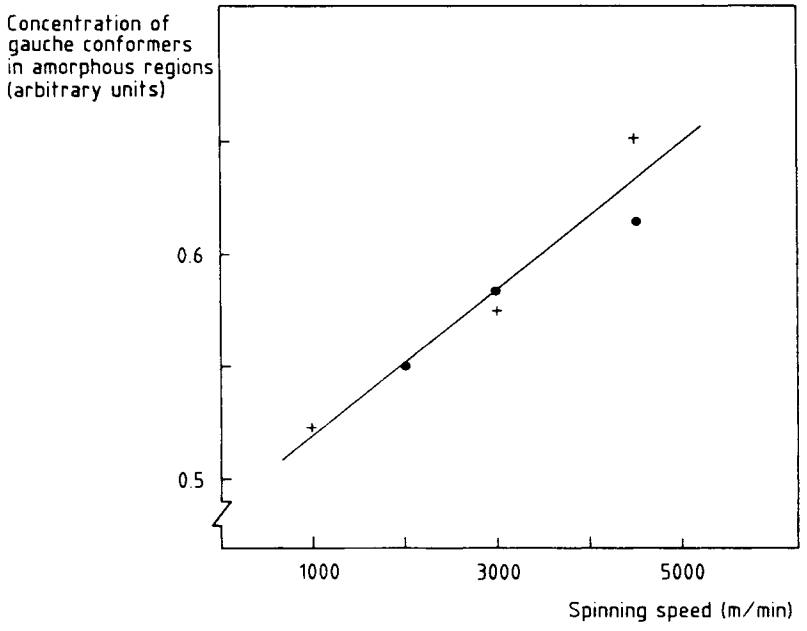

Fig. 15. Concentration of gauche conformers in amorphous regions for drawn yarns spun at various speeds: (●) high T_{draw}; (+) low T_{draw}.

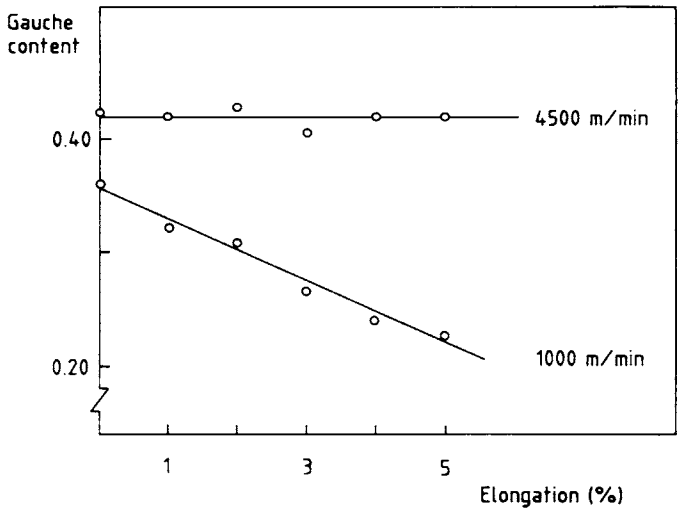

Fig. 16. Dependence of gauche content on strain for drawn yarns spun at 1000 and 4500 m/min.

m/min clearly shows that uncoiling takes place in that yarn. Contrary to this, the yarn originally spun at 4500 m/min does not show any systematic change in gauche content on straining. This means that the high-speed spun yarn contains very big loose loops that cannot be straightened upon straining to the elongations applied.

By means of curve resolution it was found that the trans absorption peak near 972 cm^{-1} was composed of a crystalline and an amorphous contribution. In Figure 17 the position of the amorphous trans absorption is plotted against the elongation. A definite decrease of position is found at increasing elongation. According to several authors[4,7,11] this shift can be ascribed to an increased stress on the taut tie-molecules. Figure 18, finally, shows the peak position just discussed in the unstrained state for yarns spun at different speeds. This fact, combined with the evidence shown in Figure 17, points to an increased stress on the taut tie molecules for the drawn yarns spun at increased speed.

Summarizing, it can be concluded that in the drawn yarns high spinning speeds give rise to an increase in folding, apparently due to the high fold content already present in the undrawn yarns,[4] in the number of big loose loops and in the stress on the taut tie molecules. The last two findings indicate broader tie chain length distributions for high-speed spun yarns. An illustration is given in Figure 19.

This model may account for the well-known decrease of tenacity for the high-speed spun yarns. As other factors leading to a decreased tenacity as reduced M_w and skin–core differences are only marginally present in this series, it is our opinion that, in this case, the decrease should be ascribed to the increased folding and the broader length distribution of tie chains.

In the discussion of the characterization methods it was stated that the overall orientation was determined by means of pulse propagation. Another

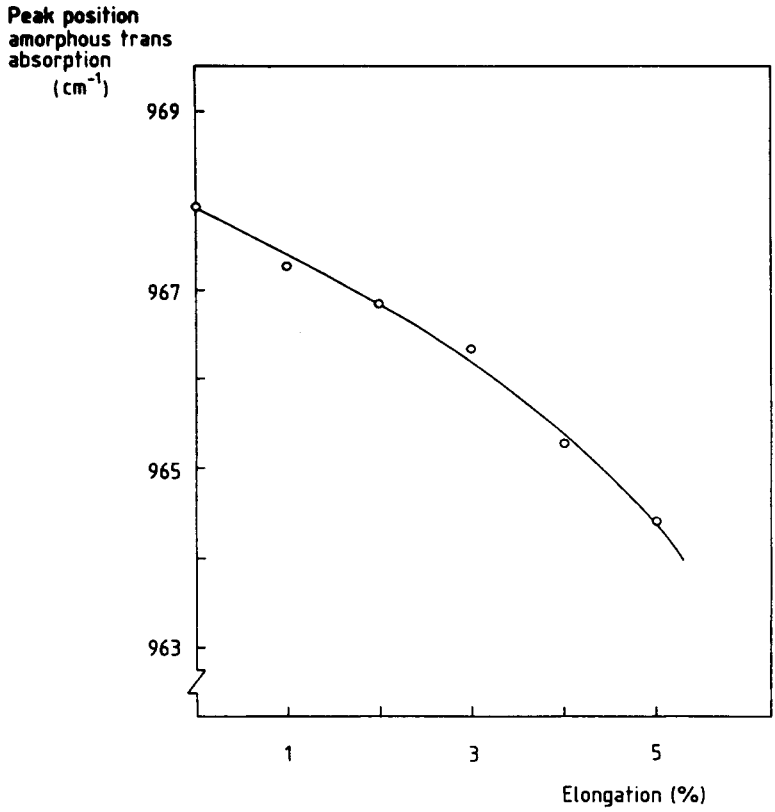

Fig. 17. Dependence of peak position of amorphous trans absorption on strain.

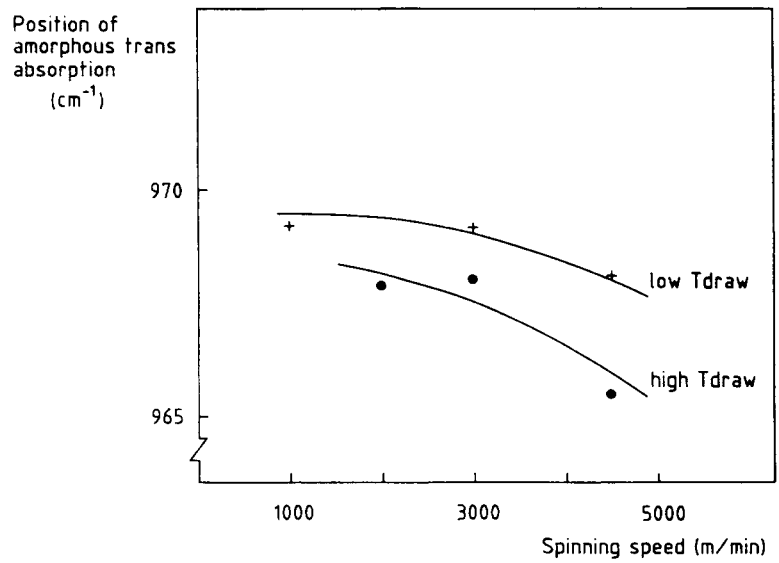

Fig. 18. Position of amorphous trans absorption for yarns spun at various speeds and drawn at different temperatures.

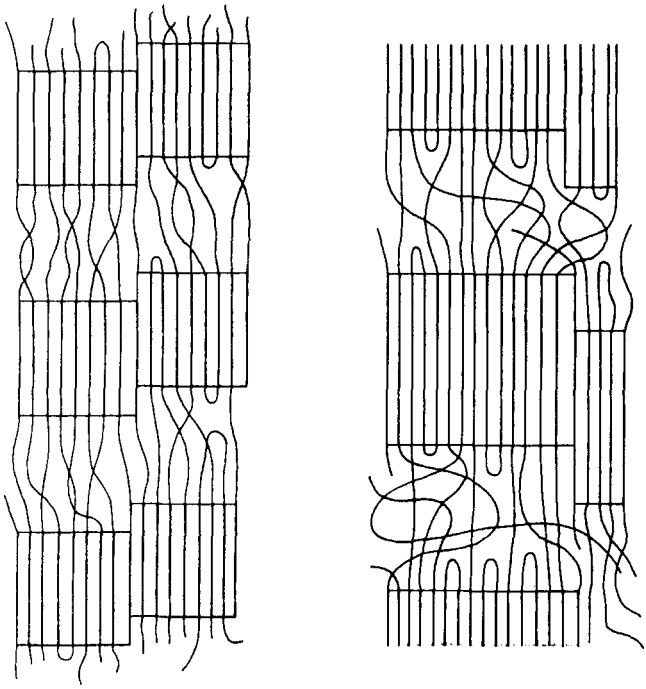

Fig. 19. Physical molecular model for drawn yarns, originally spun at (a) low speed and (b) high speed.

measure of the overall orientation is the birefringence, obtained by means of polarization microscopy. Interference microscopy showed that for this series of yarns no substantial difference between the birefringence in the skin and in the core was present. So the birefringence values can also be considered to be representative of the orientation throughout the cross section of these filaments. In Figure 20 values of sonic modulus and birefringence are plotted vs. one another for the series of yarns under discussion in this paper.

Included in the same figure are data resulting from a series of yarns obtained by thermal aftertreatment at different tensions, using one conventionally processed feeder yarn. It is clear that for the latter series there is a unique relation between sonic modulus and birefringence value. For the other yarns, however, such a unique relation cannot be established at all. Very systematic deviations can be observed from the drawn line based on the after-treated yarns.

This combination of sonic modulus and birefringence can provide more detailed information about the orientation, as both techniques give different information about the orientational distribution in the yarn. This will briefly be outlined now.

Based on the uniform stress model, Ward[12] states that

$$\frac{1}{E_{son}} = S_{11}\langle \sin^4 \phi \rangle + S_{33}\langle \cos^4 \phi \rangle + (2S_{13} + S_{44})\langle \sin^2 \phi \cos^2 \phi \rangle \quad (1)$$

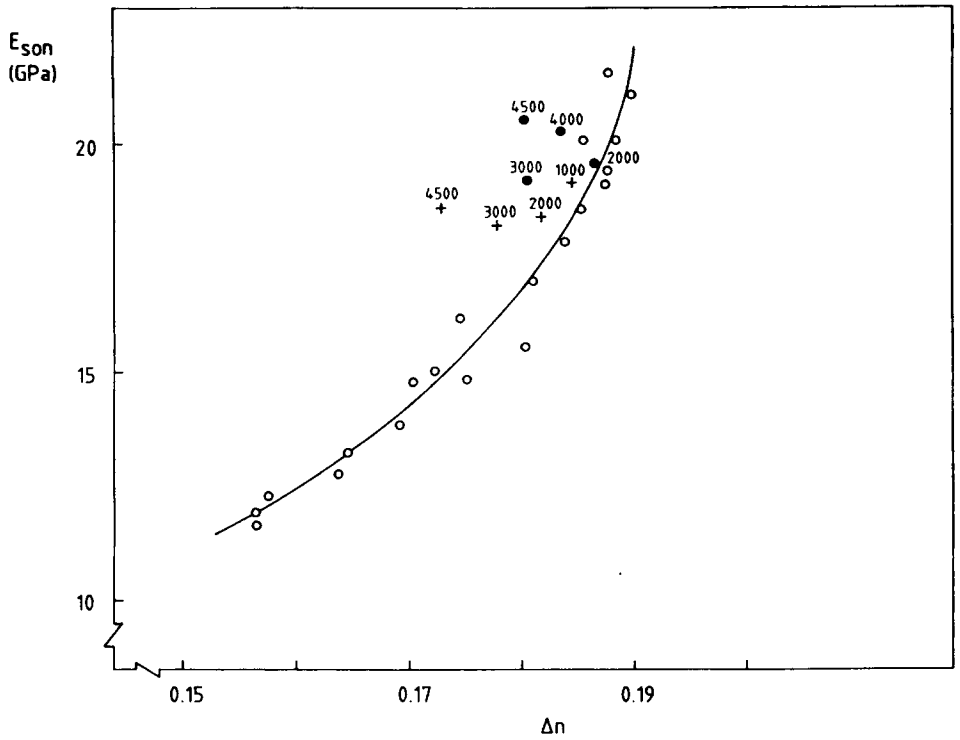

Fig. 20. Sonic modulus versus birefringence for a series of after-treated yarns (○) based on one conventionally spun feeder yarn and yarns spun at speeds (m/min) indicated in the figure and drawn at two different temperatures: (+) low draw temp; (●) high draw temp.

where ϕ = the angle between the molecular segment and the yarn axis, S_{11} = transverse compliance, S_{33} = longitudinal compliance, S_{44} = torsional compliance, and $S_{13} = \nu S_{33}$ with ν = Poisson's ratio. Assuming $\nu = 0.5$, rearrangement of eq. (1), after applying some goniometry, gives

$$\frac{1}{E_{\text{son}}} = S_{11} + \langle\cos^2\phi\rangle(-2S_{11} - S_{33} + S_{44}) + \langle\cos^4\phi\rangle(S_{11} + 2S_{33} - S_{44}) \tag{2}$$

In addition, it is known that

$$\Delta n = \tfrac{1}{2}\Delta n_{\max}(3\langle\cos^2\phi\rangle - 1) \tag{3}$$

So the birefringence measurement only reflects the second moment with respect to $\cos\phi$ of the orientational distribution. The sonic modulus, however, is related to a combination of second and fourth moment as indicated above.

From Figure 20 it follows that at the same birefringence value, i.e., $\langle\cos^2\phi\rangle$, quite a variation in sonic modulus is possible. This must be ascribed to a variation in values of the fourth moment. To consider this point in some more

detail, the derivative

$$\frac{\partial(1/E_{son})}{\partial\langle\cos^4\phi\rangle} = S_{11} + 2S_{33} - S_{44} \tag{4}$$

at constant Δn, so at constant $\langle\cos^2\phi\rangle$, is investigated. Taking for the compliances involved the values given by Ward for highly oriented PET fibers (Ref. 10, p. 248), i.e., $S_{11} = 1.6$, $S_{33} = 0.071$, and $S_{44} = 1.4$ GPa^{-1}, it appears that this derivative is positive. Consequently, lower values of $1/E_{son}$ indicate lower values of $\langle\cos^4\phi\rangle$. From Figure 20 it can be seen that lower values of $1/E_{son}$, are found for yarns spun at higher speeds. So, at higher spinning speeds, the ratio $\langle\cos^2\phi\rangle/\langle\cos^4\phi\rangle$ increases, pointing to a broader orientation distribution, as this ratio increases from 1.0 for an infinitely sharp distribution to 1.67 for a completely random one. This result is very well in line with the findings of infrared spectroscopy discussed before.

Dynamic-Mechanical Behavior Related to Structure

The dynamic-mechanical behavior of a yarn is supposed to be related to the mobility of the molecular segments in the amorphous regions. This mobility can be related to the crystalline morphology. If the crystals are regarded as physical crosslinks decreasing the segmental mobility, many small crystals will have a greater crosslinking effect than fewer bigger ones. Consequently, the molecular mobility in the amorphous domains is considered to be directly related to the volume of these regions.

In Figure 21 the lateral and longitudinal crystal sizes are plotted vs. the spinning speed for yarns drawn at the two temperatures, respectively. Another lateral crystal size, also determined by means of x-ray diffraction, is not shown here. Both effects of spinning speed and drawing temperature are clearly visible in this picture. From the two lateral crystal sizes and the longitudinal one, the average volume of a crystal, V_{CR}, can be estimated. From this information, assuming an alternating succession of crystalline and amorphous regions, the averaged volume of the amorphous regions can be calculated

$$V_{AM} = \frac{1 - V_c}{V_c} \cdot V_{CR}$$

This is the free volume introduced by Dumbleton and Murayama.[13] Vassilatos, Knox, and Frankfort[14] introduced the corrected free volume as a measure of the molecular mobility, also taking into account the amorphous orientation

$$V_F = V_{AM} \cdot \frac{1 - f_a}{f_a}$$

with f_a determined from birefringence measurements, providing a slightly better description than using pulse propagation results.

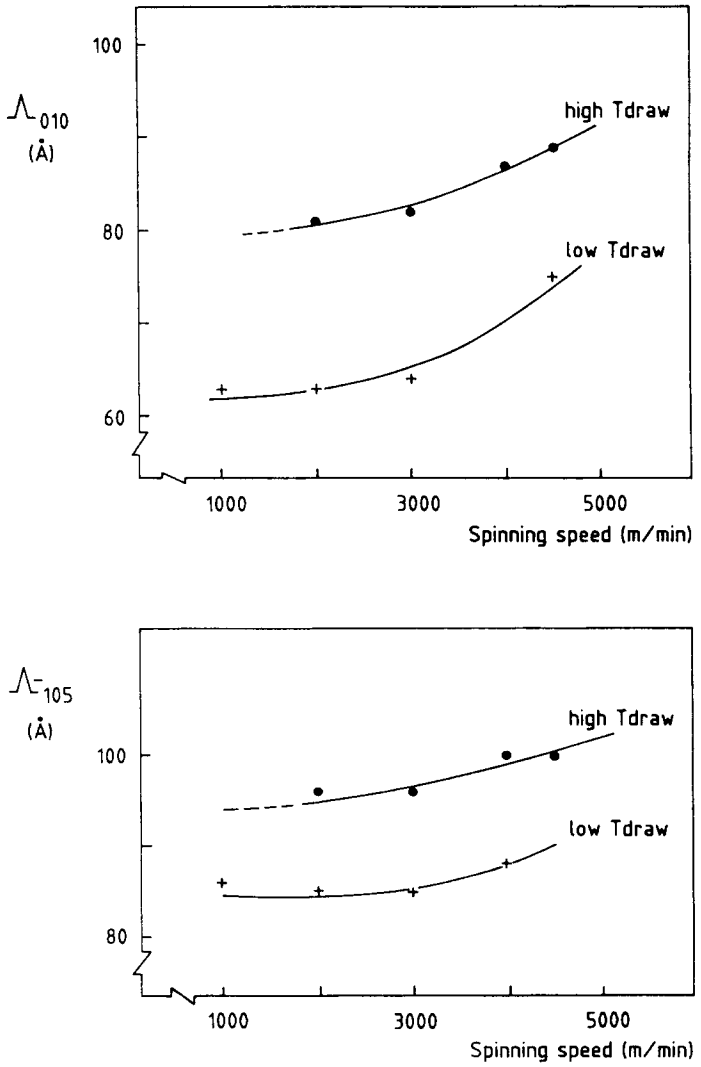

Fig. 21. Lateral and longitudinal crystal size for yarns spun at various speeds and drawn at two different temperatures.

For the present yarns this latter parameter is plotted vs. the spinning speed at two temperatures (Fig. 22). A very pronounced increase in the corrected free volume is found, with a significant contribution of the drawing temperature.

A mechanical response to the molecular mobility is the temperature where the dynamic loss modulus E'' shows a maximum, the so-called α transition temperature. In Figure 23 this transition temperature is plotted vs. the spinning speed.[15] A definite decrease is observed at increasing spinning speed, in addition to a substantial effect of the drawing temperature. This $T_{E''_{max}}$, based on the discussion just given, should be related to the corrected free volume. Figure 24 shows this relation for the yarns involved. Also a variety of other drawn and undrawn yarns was added to complete the picture. Since a

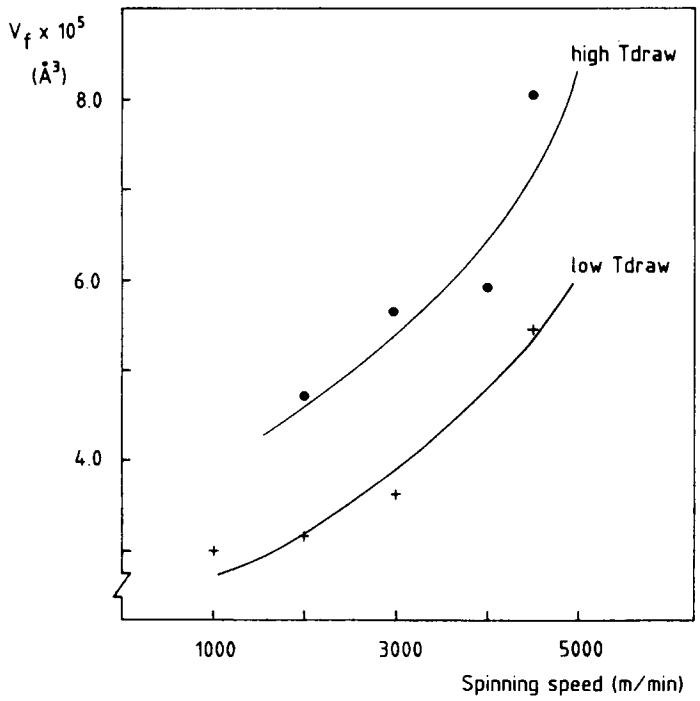

Fig. 22. Corrected free volume for yarns spun at various speeds and drawn at different temperatures.

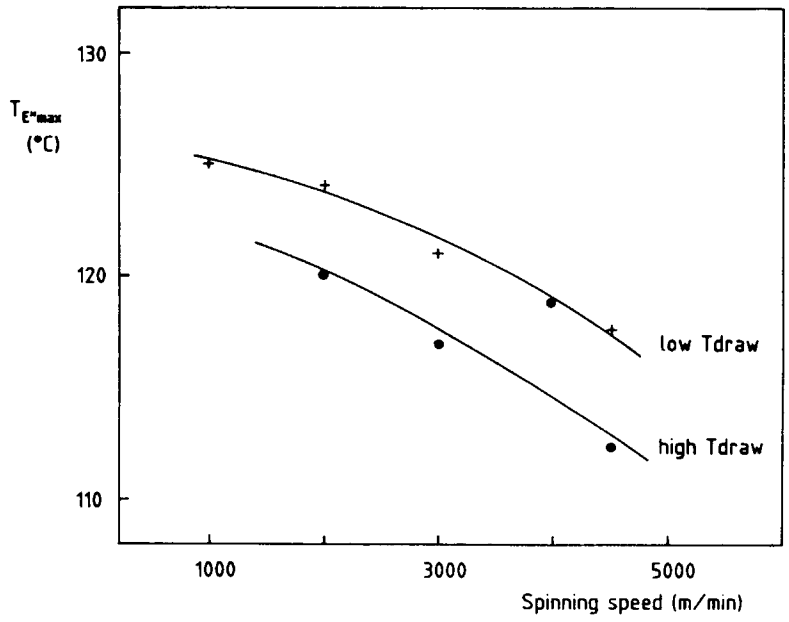

Fig. 23. Temperature of dynamic mechanical α transition for yarns spun at various speeds and drawn at different temperatures.

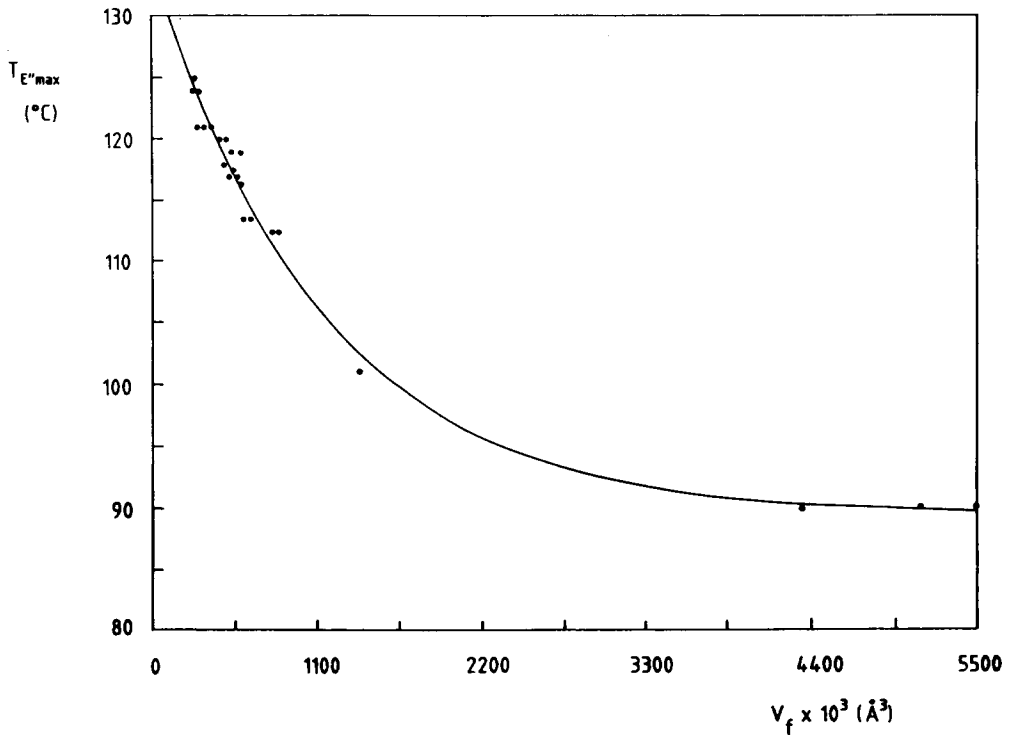

Fig. 24. Relation between temperature of α transition and corrected free volume.

very good fit is obtained, the model may be regarded as justified. A similar fit was also reported by Vassilatos et al.[14] The limiting value of $T_{E''_{max}}$ for infinitely high values of the free volume, i.e., for amorphous yarns, is 89°C. This is close to the glass transition in PET as measured by thermal methods. The mobility of the chains plays a role both in diffusional properties, such as dye absorption, and in dynamic response such as fatigue resistance.

CONCLUSION

Examples have been presented to show that quantitative information, deduced from a simple two-phase model for PET yarns, can suitably be used for describing the mechanical yarn properties. The physical understanding of these properties can be improved in this way; consequently, the changes in mechanical properties brought about by changes in process conditions can better be understood and predicted. Therefore, from an industrial point of view, this kind of structure investigation is a very effective application of polymer science.

The authors gratefully acknowledge the cooperation with A. Roos, for providing the yarns, performing the dynamic mechanical work, and discussing the results, L. J. Lucas, for performing and interpreting the measurements of the mechanical properties, H. Mannee, for his substantial contribution to this kind of work by developing so many sophisticated but yet user-friendly computer programs, H. H. W. Feijen, for the lively discussions, and A. Bezemer and J. M. Woestenenk, who supported and strongly encouraged this type of work from the very beginning.

References

1. R. J. Samuels, *Structured Polymer Properties*, Wiley, New York, 1974.
2. R. Huisman and H. M. Heuvel, *J. Appl. Polym. Sci.*, **22**, 943 (1978).
3. H. M. Heuvel and R. Huisman, *J. Appl. Polym. Sci.*, **22**, 2229 (1978).
4. H. M. Heuvel and R. Huisman, *J. Appl. Polym. Sci.*, **30**, 3069 (1985).
5. L. J. Lucas, *Text. Res. J.*, **53**, 771 (1983).
6. W. O. Statton, J. L. Koenig, and M. Hannon, *J. Appl. Phys.*, **41**, 4290 (1970).
7. S. N. Zhurkov, V. I. Vettegren, I. I. Novak, and K. N. Kashincheva, *Dokl. Akad. Nauk USSR*, **176**, 623 (1967).
8. I. M. Ward, *Chem. Ind.*, 905 (1956).
9. I. M. Ward, *Chem. Ind.*, 1102 (1957).
10. D. Grime and I. M. Ward, *Trans. Faraday Soc.*, **54**, 959 (1958).
11. K. K. R. Mocherla and W. O. Statton, *J. Appl. Polym. Sci., Appl. Polym. Symp.*, **31** 183 (1977).
12. I. M. Ward, *Mechanical Properties of Solid Polymers*, Wiley-Interscience, London, 1971, p. 254.
13. J. H. Dumbleton and T. Murayama, *Koll. Z. Z. Polym.*, **220**, 41 (1967).
14. G. Vassilatos, B. H. Knox, and H. R. E. Frankfort, in *High-Speed Fiber Spinning*, A. Ziabicki and H. Kawai, Eds., Wiley-Interscience, New York, 1985.
15. A. Roos, unpublished results.

Received November 3, 1987
Accepted January 15, 1988